

Effect of Welding Process and Different Stress Conditions on Electrochemical Noise Characterization of Ti-6Al-4V Alloy

Yan Liu^{1,*}, Jicai Feng², Shuping Tan¹, Yi Cheng¹, Jin Hu^{3,*}

¹ State Key Laboratory of Efficient and Clean Coal-Fired Utility Boilers, Harbin Boiler Company Limited, Harbin 150046, China

² State Key Laboratory of Advanced Welding and Joining, Harbin Institute of Technology, Harbin 150001, China

³ School of Materials Science and Engineering, Harbin Institute of Technology, Harbin 150001, China

*E-mail: liuyan_research@yeah.net, hujin@hit.edu.cn

Received: 10 April 2020 / Accepted: 5 June 2020 / Published: 10 August 2020

The electrochemical noise characterization of Ti-6Al-4V alloy before and after the welding process has been investigated. Electrochemical noise measurements are always simultaneously performed on two identical samples: one sample for the non-stressed test and the other sample for the slow-strain-rate tensile test. The difference in surface state between non-welded and welded samples is the main reason for the change in electrochemical characteristics. The welded sample has high corrosion sensitivity under the non-stressed state and slow-strain-rate tensile tests. The application of an external force promotes the electrochemical corrosion process of the sample before and after the welding process.

Keywords: Electrochemical noise; Ti-6Al-4V alloy; Welding process; Slow-strain-rate tensile test

1. INTRODUCTION

Titanium alloys have excellent chemical compatibility and mechanical properties and are widely used in nuclear, aviation, medical, chemical, civil and other fields similar to steel [1-5]. In addition, due to the formation of titanium dioxide (TiO₂) on the surface, titanium alloys show excellent corrosion resistance in corrosion media [6-8]. The TiO₂ thin layer is dense and stable, which can protect the metal from continuous oxidation [9,10]. However, external conditions such as the combined action of acidic environment and abnormal cyclic loads cause the rupture and permanent failure of the protective oxide film [11,12]. Therefore, the matrix metal may be exposed to the corrosion medium [13]. There are many studies on the stress corrosion cracking of titanium alloys that show that titanium alloys are prone to stress corrosion cracking in different environments [14-19].

Welding has been an indispensable technical method in the processing and manufacturing of titanium alloy products [20-24]. For titanium alloy weldments, the welding process has an adverse effect on the corrosion resistance [25,26]. Since the martensite phase transformation may occur in the weld zone and heat affected zone during the titanium alloy welding process, the corrosion behavior is strongly affected by the change in crystal structure, so the corrosion resistance of the weld is worse than that of the base metal. Thus, the weld zone is considered extraordinarily sensitive to corrosion because of its special structure compared to the base metal [27,28]. Unfortunately, in the corrosive environment that may lead to stress corrosion cracking of titanium alloys, there are very few studies on the difference of corrosion behavior characterization between non-welded and welded titanium alloys under external stress. There is excellent corrosion resistance for titanium alloy in aqueous solutions, but under the action of the applied stress, especially in the presence of chloride such as LiCl, corrosion will occur in organic environments such as anhydrous methanol and propanol media [14,15,29,30].

As known to all, electrochemical noise has been considered an effective research method for the electrochemical corrosion process and widely applied in various metal materials, which can be used to study the key information of the reaction process on the electrode [31-34]. Electrochemical noise has been combined with the slow-strain-rate tensile test for the corrosion research of steel and gold-copper alloy [35-38], but there is almost no related research on titanium alloy and its weldment. In this paper, the slow-strain-rate tensile test and non-stressed loading test were used to study the electrochemical noise characterization of Ti-6Al-4V alloy with and without a welding process.

2. EXPERIMENTAL

2.1 Materials

In this work, Ti-6Al-4V alloy plates (240 mm length \times 50 mm width \times 1 mm thickness) with the chemical compositions in Table 1 were prepared.

Table 1. Chemical compositions (mass%) of Ti-6Al-4V alloy plates.

Element	Al	V	Fe	Si	C	O	H	N	Ti
Content	5.9	4.0	0.08	0,005	0.02	0.1	0.002	0.03	Balance

2.2 Welding process

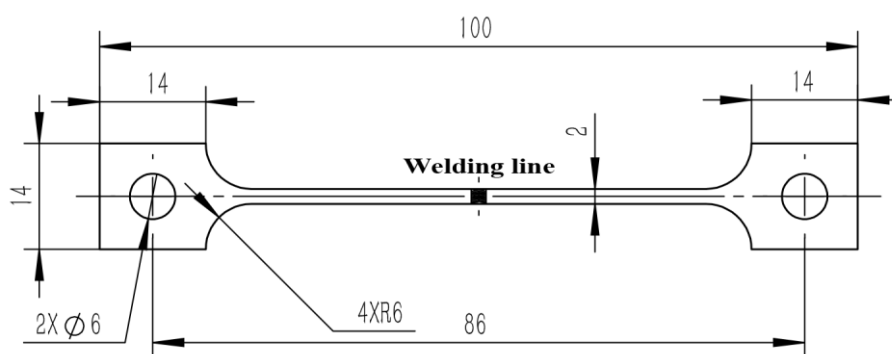
An ROFIN-DC030 laser beam system was employed to weld all Ti-6Al-4V alloy joints with the welding process parameters in Table 2.

Table 2. Welding process parameters of Ti-6Al-4V alloy plates.

Parameters	Power (W)	Frequency (Hz)	Welding speed (m/min)	Argon pressure (MPa)
Value	800	35	1	0.12

2.3 Slow-strain-rate tensile test

Slow-strain-rate tensile tests with a strain rate of 3×10^{-7} /s were performed on non-welded and welded Ti-6Al-4V alloys in air and LiCl-CH₃OH solution (0.1 mol/L), respectively. The dimensions of the samples in the slow-strain-rate tensile test are shown in Figure 1.

**Figure 1.** Dimensions of the samples in the slow-strain-rate tensile test, mm.

2.4 Electrochemical measurements

The Gamry Reference 3000 electrochemical workstation was selected to measure the electrochemical noise in the slow-strain-rate tensile test. The improved electrochemical noise technology "Electrochemical Emission Spectroscopy" was used for testing, the reference electrode was an Ag/AgCl/CH₃OH electrode, the working electrode was the sample to be tested, and the counter electrode was a platinum microcathode [38-43]. No bias voltage was applied to the tensile sample in the electrochemical noise test, and the sampling frequency was 10 Hz.

3. RESULTS AND DISCUSSION

3.1 Slow-strain-rate tensile test and stress corrosion cracking sensitivity

The slow-strain-rate tensile test has been recognized as an effective method to evaluate the stress corrosion cracking sensitivity, which was applied to the non-welded and welded Ti-6Al-4V alloy samples in this study [44-47]. Figure 2 and Table 3 present the stress-strain curves and mechanical properties obtained from the slow-strain-rate tensile test of non-welded and welded samples in air and LiCl-CH₃OH solution; thus, the stress corrosion cracking sensitivity of the samples can be described.

There are few differences in mechanical properties between non-welded sample and welded sample in air, but the mechanical properties of the welded sample are significantly lower than those of the non-welded sample in the corrosion medium.

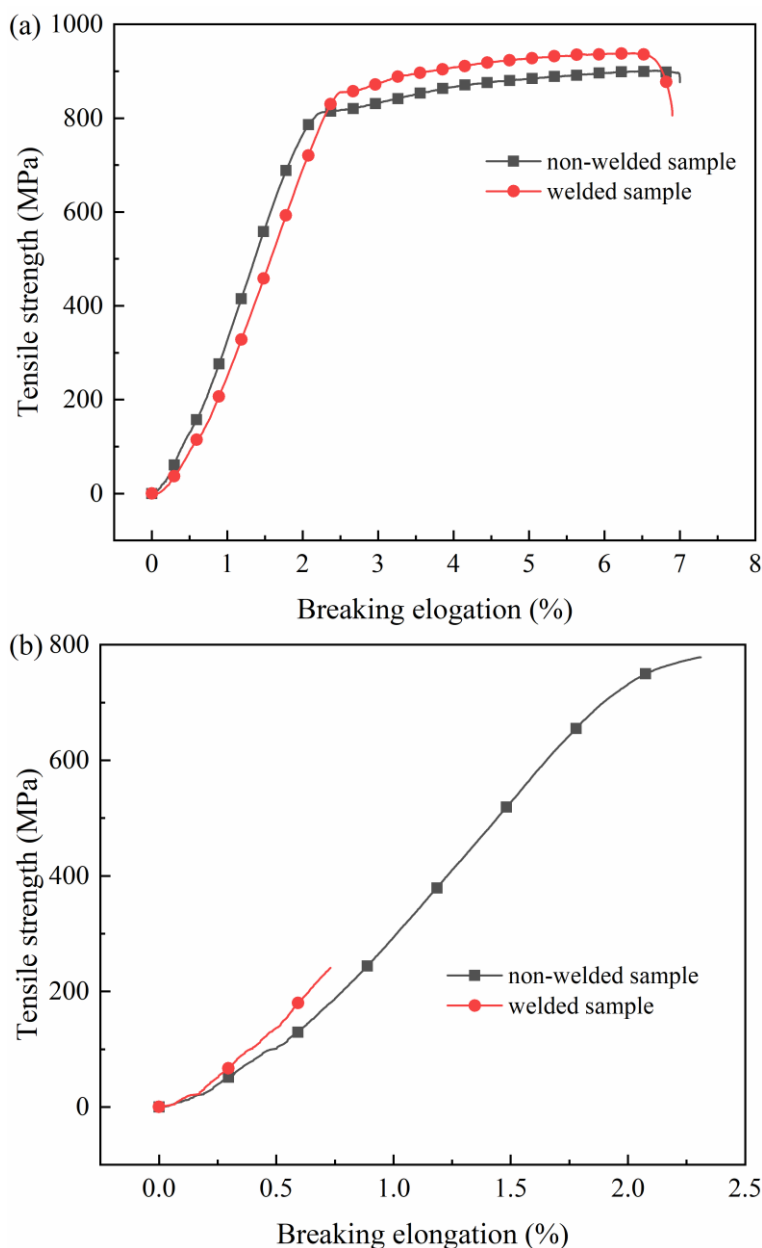


Figure 2. Stress-strain curves of non-welded and welded Ti-6Al-4V alloys obtained from the slow-strain rate tensile test in air and 0.1 mol/L LiCl-CH₃OH solution: (a) samples tested in air; (b) samples tested in 0.1 mol/L LiCl-CH₃OH solution.

The mechanical properties of non-welded samples in the corrosion medium are lower than those in air, which indicates that the Ti-6Al-4V alloy has a certain stress corrosion cracking sensitivity. However, the mechanical properties of welded samples in the corrosion medium are far lower than those in air, which indicates that the welded Ti-6Al-4V alloy has a relatively high sensitivity to stress corrosion cracking. The results of this study have been confirmed by other related studies, which applied the slow-

strain-rate tensile test to Ti-6Al-4V alloy in CH₃OH solution and air and found a 52.1% reduction in the breaking elongation of the sample tested in the CH₃OH solution compared to the sample tested in air [48].

For non-welded and welded Ti-6Al-4V alloys, the stress corrosion cracking sensitivity can be characterized by the sensitivity index, which is expressed by the loss ratio of mechanical properties obtained from the slow-strain-rate tensile test in air and LiCl-CH₃OH solution [44]. The sensitivity index can be calculated using the following formula:

$$I_{\sigma} (\%) = \frac{\sigma_{air} - \sigma_{sol}}{\sigma_{air}} \times 100 \quad (1)$$

$$I_{\epsilon} (\%) = \frac{\epsilon_{air} - \epsilon_{sol}}{\epsilon_{air}} \times 100 \quad (2)$$

where I_{σ} and I_{ϵ} are the sensitivity index of strength and plasticity, σ_{air} and σ_{sol} are the tensile strength obtained from the samples tested in air and LiCl-CH₃OH solution, and ϵ_{air} and ϵ_{sol} are the breaking elongation obtained from the samples tested in air and LiCl-CH₃OH solution [45,47].

Table 3. Mechanical properties obtained from the slow-strain-rate tensile test of non-welded and welded Ti-6Al-4V alloys in air and 0.1 mol/L LiCl-CH₃OH solution.

State	Condition	Tensile strength (MPa)	Breaking elongation (%)
Non-welded sample	Air	901	7.01
Non-welded sample	LiCl-CH ₃ OH solution	778	2.31
Welded sample	Air	937	6.91
Welded sample	LiCl-CH ₃ OH solution	241	0.73

Using the mechanical properties in Table 3, we conclude that I_{σ} and I_{ϵ} for the non-welded samples are 13.65% and 67.05%, and I_{σ} and I_{ϵ} for the welded samples are 74.28% and 89.43%, respectively. The results show that the welded sample has a much higher sensitivity index than the non-welded sample. A related study found that the plastic sensitivity index of Ti-6Al-4V alloy in an HCL-CH₃OH solution was 52.1% and 92.5% during the slow-strain-rate tensile test, which is similar to the result of this study [48,49].

These results indicate that the welding process greatly enhances the stress corrosion cracking sensitivity of Ti-6Al-4V alloy in LiCl-CH₃OH solution, which is mainly attributed to the change in corrosion resistance of the Ti-6Al-4V alloy before and after welding [50]. Our previous study tested the potentiodynamic polarization curves of Ti-6Al-4V alloy before and after the welding process and found that the two samples had different electrochemical behaviors. For the non-welded sample, the anodic current density slowly increased with the increase in polarization potential, and the anodic polarization curve showed an obvious passivation zone. For the welded sample, the anodic current density rapidly increased with increasing polarization potential, and there was a relatively low pitting potential in the anodic polarization curve. The results show that the welding process resulted in poor corrosion resistance of the Ti-6Al-4V alloy weldment because there was a welding seam that deteriorated the protective performance of the oxide film on the surface of the sample [50]. Our previous results are consistent with

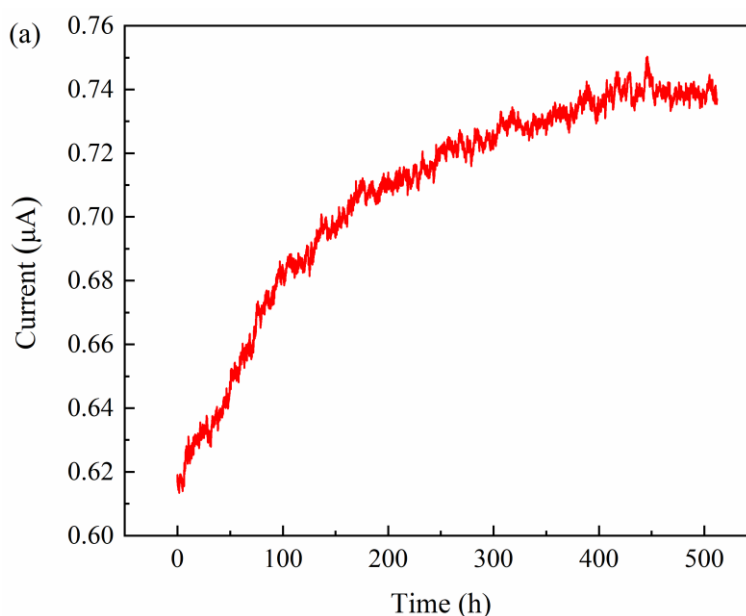
the results of some electrochemical corrosion studies on Ti-6Al-4V alloy and its weldment [25-29,48]. In related studies, the polarization curves of Ti-6Al-4V alloy were measured in HCl-CH₃OH solution and LiCl-C₃H₇OH solution, and the passivation phenomena were similar to that in the polarization curve in our previous study [29,48]. The Ti-6Al-4V alloy showed good local corrosion resistance in corrosion media because it was protected by a natural oxide film on its surface [6-10]. For the welded sample of Ti-6Al-4V alloy, relevant studies have found that the corrosion potential in corrosion media was -0.24 V (the corrosion potential obtained in our previous study was -0.16 V), the anodic current density significantly increased with the increase in polarization potential, and the anodic polarization curve presented a relatively low pitting potential [25-28].

3.2 Removal of the direct current component in the electrochemical noise signal

Before analyzing the electrochemical noise data, a suitable method must be used to remove the direct current component of the original noise signal [38,51-53]. The polynomial fitting method is a relatively effective method to remove the direct current components [51]. Taking the current noise signal as an example, the following relations are mainly followed when the polynomial fitting method is used to remove the direct current components:

$$I = I_0 + a_0 + a_1t + a_2t^2 + a_3t^3 + \dots + a_nt^n \quad (3)$$

where I is the original current noise signal, and I_0 is the real current noise signal [51]. Studies have shown that when the highest power of the polynomial fitting method is 5, the direct current component in the original noise signal can be completely removed. The real signal required is simultaneously retained to the greatest extent, which ensures that the effective information in the real signal is not weakened or eliminated [51]. Thus, the quintic polynomial fitting method was selected to remove the direct current component of the original electrochemical noise data in this study.



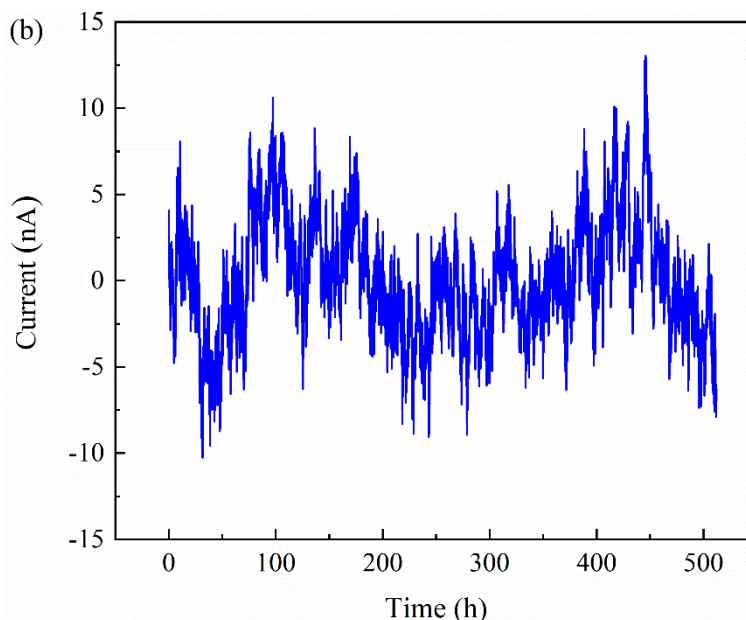


Figure 3. Current noise signal of the non-welded Ti-6Al-4V alloy obtained from the initial stage of the non-stressed immersion test in 0.1 mol/L LiCl-CH₃OH solution before and after the direct current component was removed: (a) original noise signal before the direct current component was removed; (b) real noise signal after the direct current component was removed.

Taking the non-welded Ti-6Al-4V alloy as an example, Figure 3 shows the current noise signal obtained from the initial stage of the non-stressed immersion test before and after the direct current component was removed. The distribution of the original noise signal obviously changes after we eliminated the direct current component, and the treated current noise signal fluctuated around the zero point, which indicates that the removal of the direct current component in the signal is reasonable [51].

3.3 Time domain analysis of the electrochemical noise signal

For electrochemical noise signals, the time domain analysis mainly refers to the analysis of signals in the time domain spectrum using mathematical statistics [53]. At present, the most commonly used analysis parameters are the electrochemical noise resistance R_n , skewness coefficient S_k and kurtosis coefficient K_u . The electrochemical noise resistance R_n is the ratio of the standard deviation of potential noise to the standard deviation of current noise [54]. Taking the current noise signal as an example, the standard deviation is defined as follows:

$$S = \sqrt{\frac{1}{n-1} \sum_{i=1}^n \left(x_i - \frac{1}{n} \sum_{i=1}^n x_i \right)^2} \tag{4}$$

where x_i is the measured transient value of the current noise signal, and n is the number of sampling points [55]. Related studies have shown that R_n is comparable to the polarization resistance, and R_n can usually be used to characterize the corrosion resistance of the material in a corrosion medium. A higher R_n indicates a better corrosion resistance, a slower corrosion rate and a milder corrosion

process, while a lower R_n represents the worse corrosion resistance, faster corrosion rate and more serious corrosion process [38,53-56].

Figure 4 shows the electrochemical noise resistance R_n of the non-welded Ti-6Al-4V alloy with testing time from the non-stressed state and slow-strain-rate tensile test. Different external stress states have great effects on R_n of the sample. R_n under the non-stressed state is high and basically remains unchanged, which indicates that the corrosion resistance of the sample is not affected by the external corrosion medium during the immersion process and is always at a high level. During the slow-strain-rate tensile test, R_n gradually decreases with the extension of testing time, which implies that the corrosion resistance of the sample gradually deteriorates under the action of the applied load. These differences are mainly caused by the differences in properties of the oxide film on the surface of the samples under different loading conditions [50]. The properties of the oxide film under the non-stressed state are very stable, and the protection performance is excellent, so the corrosion resistance of the sample in the corrosion medium is excellent and does not significantly change [6-10]. Under the continuous action of an applied load during the slow-strain-rate tensile test, the stability of the oxide film worsens, the compactness of the oxide film decreases, and the protective ability of the oxide film to the sample continuously decreases, which causes the stress corrosion cracking of the sample during the slow-strain-rate tensile test [50,57,58].

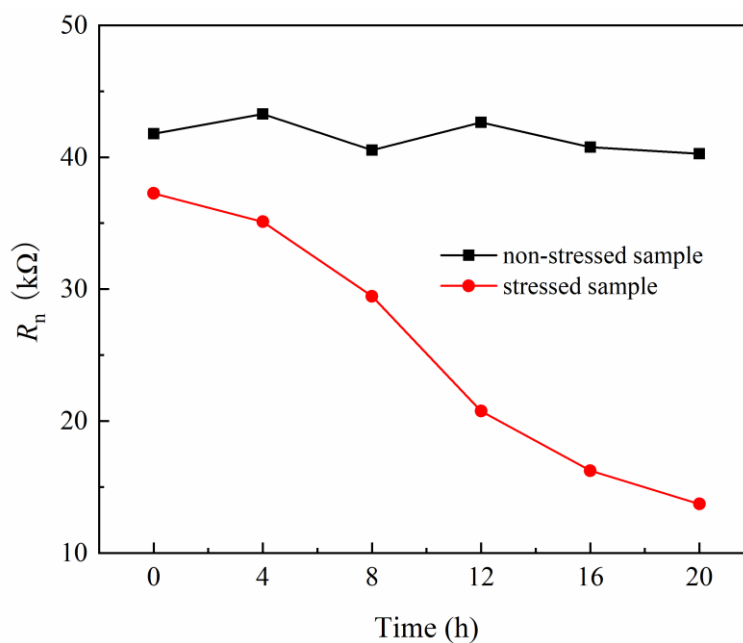


Figure 4. Electrochemical noise resistance R_n of the non-welded Ti-6Al-4V alloy with testing time from the non-stressed state and slow-strain-rate tensile test in 0.1 mol/L LiCl-CH₃OH solution.

The electrochemical noise resistance R_n of the welded Ti-6Al-4V alloy with testing time in the non-stressed state and slow-strain-rate tensile test is shown in Figure 5. There is no obvious change in R_n of the non-stressed sample, which indicates that the corrosion medium does not significantly affect the corrosion resistance of the sample. R_n of the sample continuously decreases with the testing time

during the slow-strain-rate tensile test, which indicates that the corrosion resistance of the sample is constantly destroyed by the applied stress during the process of stress corrosion cracking. Under the non-stressed state, the non-welded sample in Figure 4 always has greater R_n than the welded sample in Figure 5, which is mainly determined by the difference in properties of the oxide film on the surface of the sample before and after the welding process for the aforementioned reasons [50].

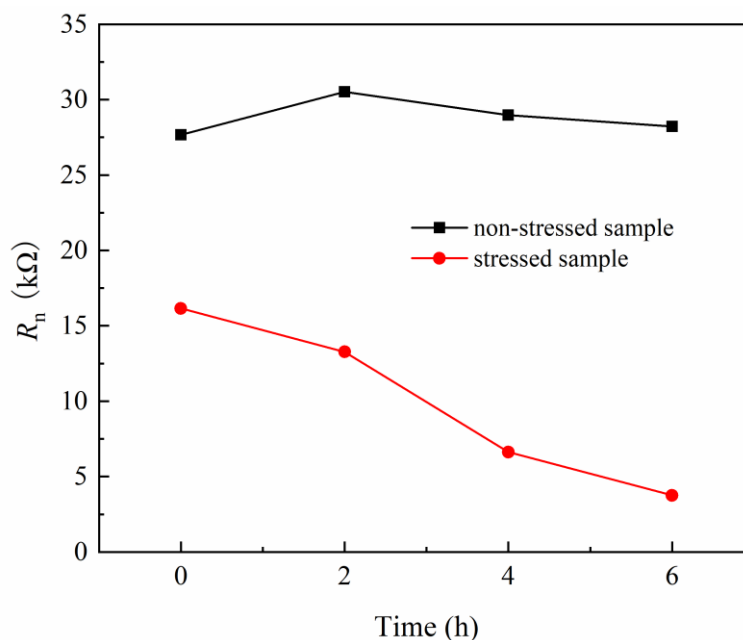


Figure 5. Electrochemical noise resistance R_n of the welded Ti-6Al-4V alloy with testing time in the non-stressed state and slow-strain-rate tensile test in 0.1 mol/L LiCl-CH₃OH solution.

In the time domain analysis, the skewness coefficient S_k and kurtosis coefficient K_u of the electrochemical noise signal are also analyzed, which are high-order statistical parameters to measure the degree of deviation from symmetry and steepness of the electrochemical noise signal distribution, respectively [59]. Taking the current noise signal as an example, the mathematical definition is shown the following formula:

$$S_k = \frac{1}{(n-1)S^3} \sum_{i=1}^n (x_i - \bar{x})^3 \tag{5}$$

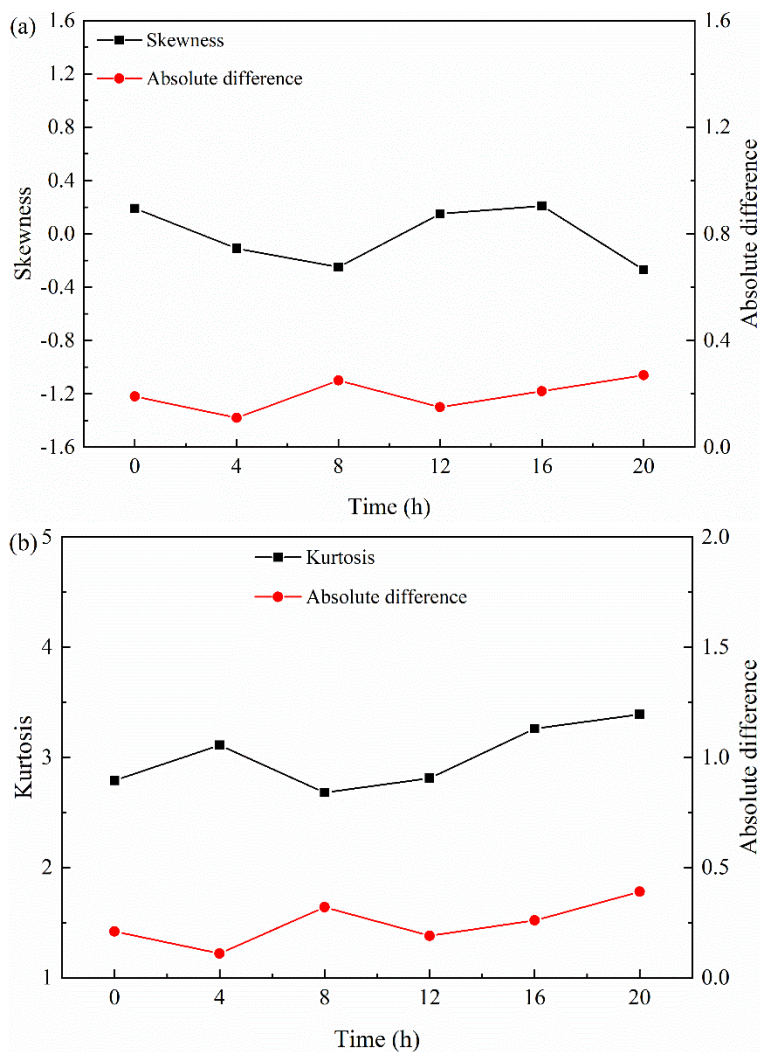
$$K_u = \frac{1}{(n-1)S^4} \sum_{i=1}^n (x_i - \bar{x})^4 \tag{6}$$

where S is the standard deviation of the current noise signal, x_i is the measured transient value of the current noise signal, \bar{x} is the average value of the current noise signal, and n is the number of sampling points. The related studies have shown that a greater difference between S_k and 0 or between K_u and 3 always indicates a faster corrosion rate and a worse corrosion resistance of the material [60].

Figure 6 exhibits the skewness coefficient S_k and kurtosis coefficient K_u of non-welded Ti-6Al-4V alloy with testing time in the non-stressed state and slow-strain-rate tensile test. The absolute

differences between S_k and 0 and between K_u and 3 are also shown in the Figure 6. There is no significant variation in absolute difference of S_k and K_u under the non-stressed state; the absolute difference is small, which indicates that the corrosion rate of the sample is slow and the corrosion resistance is high. The absolute difference of S_k and K_u gradually increases during the slow-strain-rate tensile test, which indicates that the corrosion resistance of the sample continuously decreases.

The skewness coefficient S_k and kurtosis coefficient K_u of welded Ti-6Al-4V alloy with testing time in the non-stressed state and slow-strain-rate tensile test are shown in Figure 7. The figure also shows the absolute differences between S_k and 0 and between K_u and 3. The absolute difference of S_k and K_u does not obviously change under the non-stressed state, which indicates that the corrosion medium hardly affects the corrosion resistance of the sample. During the slow-strain-rate tensile test, the absolute difference of S_k and K_u increases with the testing process, which indicates that the corrosion rate of the sample increases, the corrosion resistance decreases, and the corrosion process becomes more intense.



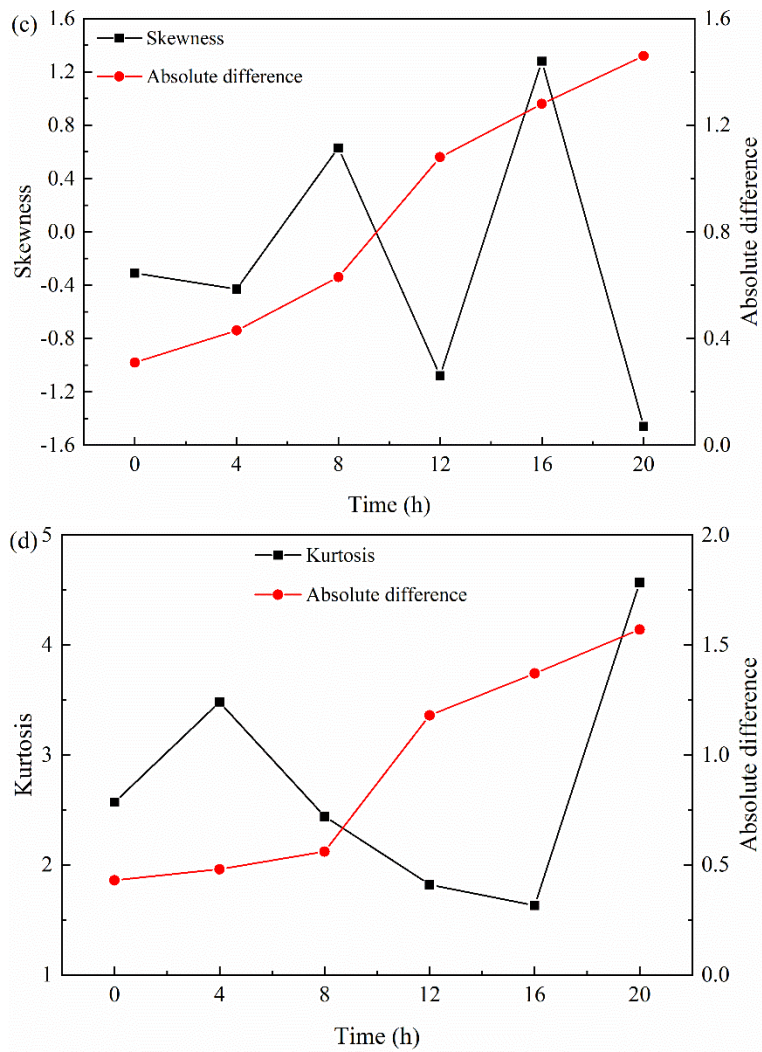
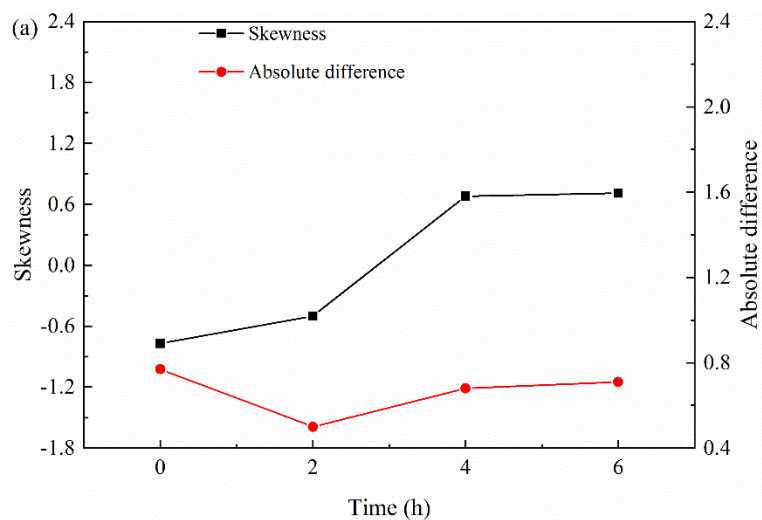


Figure 6. Skewness coefficient S_k and kurtosis coefficient K_u (absolute differences between S_k and 0 and between K_u and 3) of non-welded Ti-6Al-4V alloy with testing time in the non-stressed state and slow-strain-rate tensile test in 0.1 mol/L LiCl-CH₃OH solution: (a,b) S_k , K_u and absolute difference of sample tested under the non-stressed state; (c,d) S_k , K_u and absolute difference of sample tested during the slow-strain-rate tensile test.



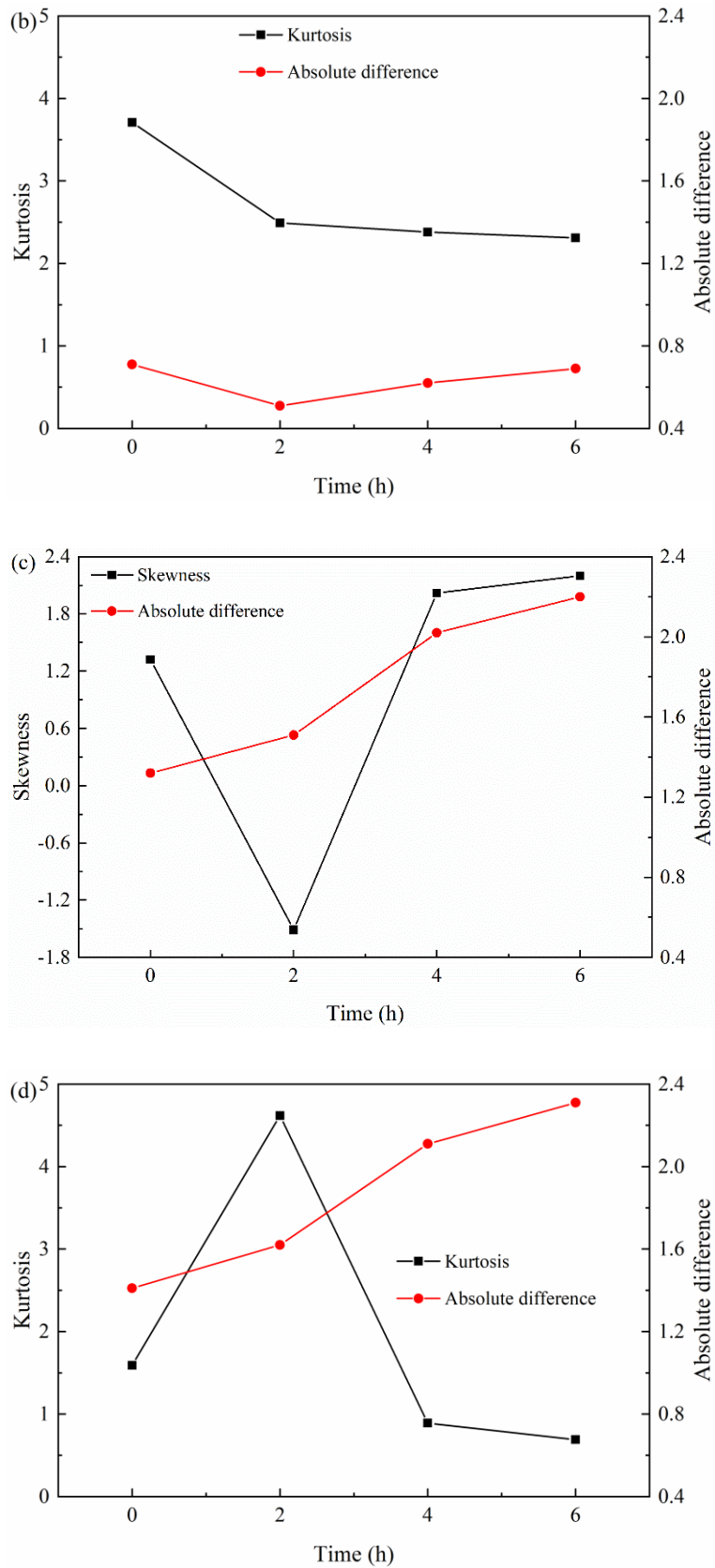


Figure 7. Skewness coefficient S_k and kurtosis coefficient K_u (absolute differences between S_k and 0 and between K_u and 3) of welded Ti-6Al-4V alloy with testing time in the non-stressed state and slow-strain-rate tensile test in 0.1 mol/L LiCl-CH₃OH solution: (a,b) S_k , K_u and absolute difference of sample tested under the non-stressed state; (c,d) S_k , K_u and absolute difference of sample tested during the slow-strain-rate tensile test.

Regardless of whether the sample has been welded or subjected to an external load, the results obtained using the absolute differences of the skewness coefficient and kurtosis coefficient are completely consistent with those obtained using the noise resistance. The results obtained by the two analysis methods can support by each other, which also shows that the conclusions of this study are accurate and reliable.

3.4 Frequency domain analysis of the electrochemical noise signal

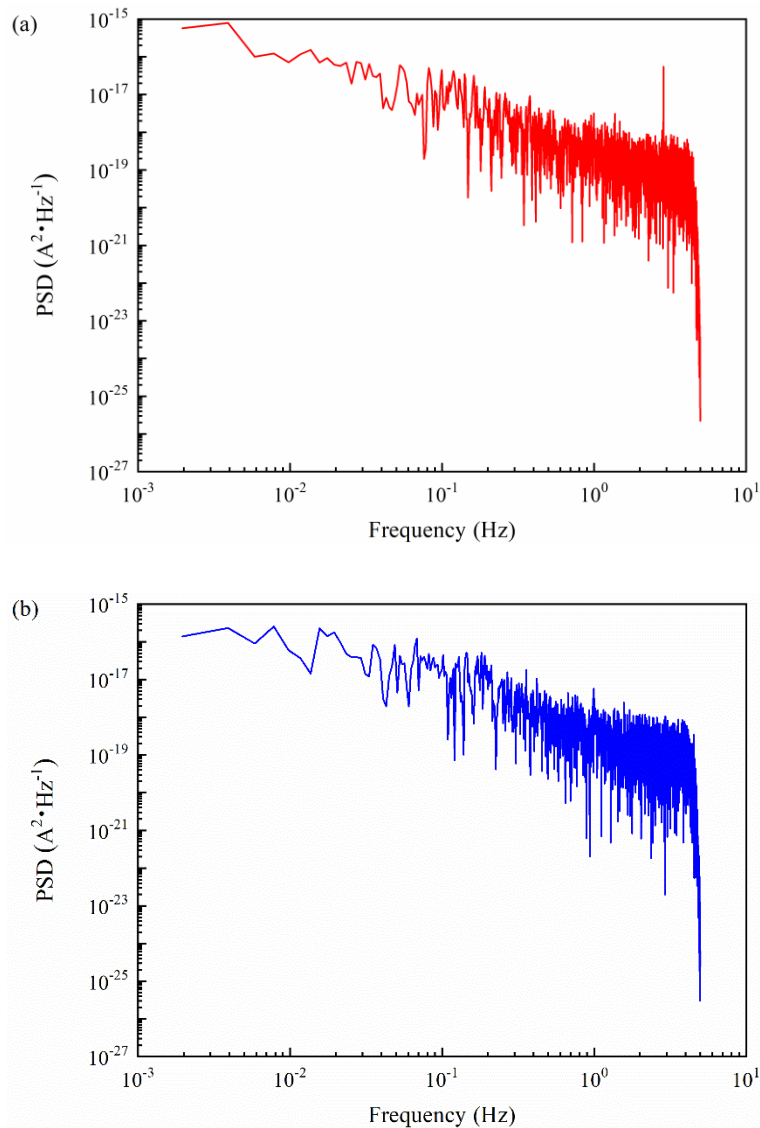


Figure 8. Frequency domain spectrum of the current noise signal of non-welded and welded Ti-6Al-4V alloys obtained from the initial stage of the non-stressed immersion test in 0.1 mol/L LiCl-CH₃OH solution: (a) frequency domain spectrum of the non-welded sample; (b) frequency domain spectrum of the welded sample.

For electrochemical noise signals, the frequency domain analysis mainly analyzes the curve of power spectral density (PSD) in the frequency domain spectrum. The slope can be obtained by linear-

fitting the PSD curve and characterize the corrosion type and corrosion tendency related to the electrode reaction process [38,51,53,56,61-63]. Taking the current noise signal as an example, Figure 8 shows the frequency domain spectrum of the non-welded and welded Ti-6Al-4V alloys obtained from the initial stage of the non-stressed immersion test.

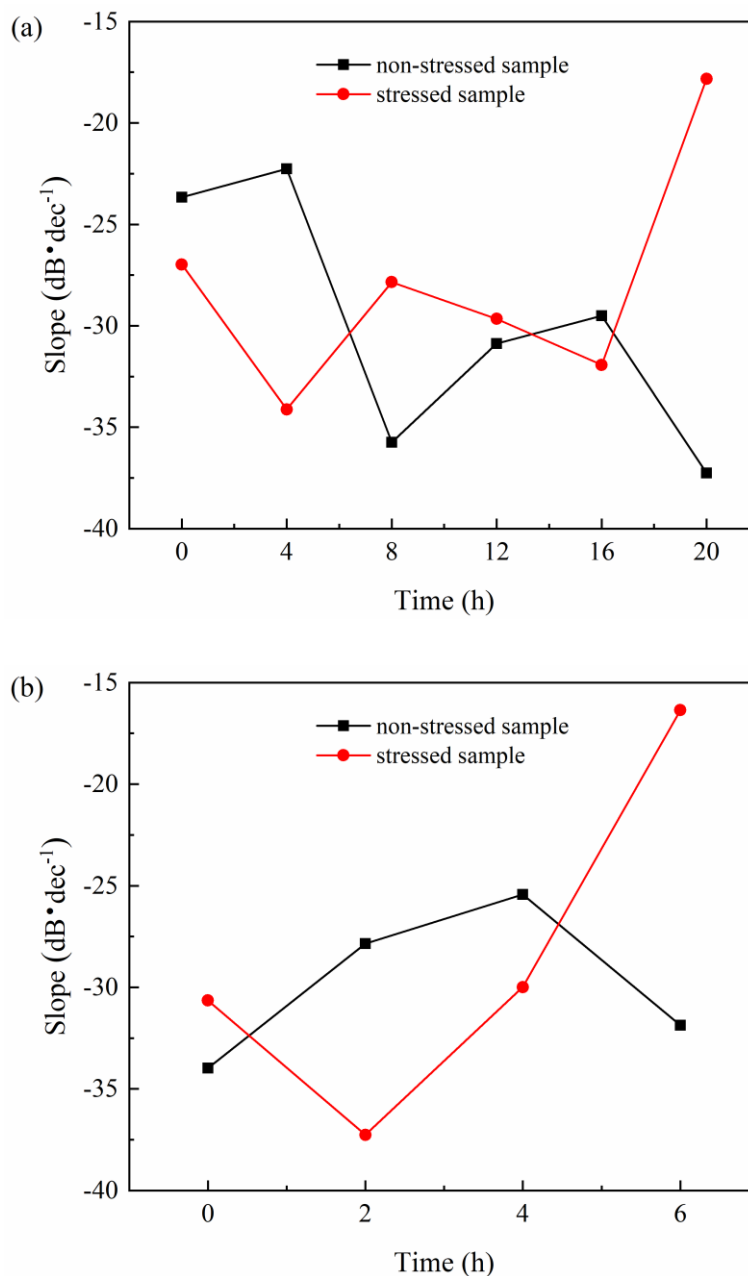


Figure 9. PSD curve slope of the current noise signal of non-welded and welded Ti-6Al-4V alloys with testing time in the non-stressed state and slow-strain-rate tensile test in 0.1 mol/L LiCl-CH₃OH solution: (a) PSD curve slope of the non-welded sample; (b) PSD curve slope of the welded sample.

Figure 9 exhibits the PSD curve slope of the current noise signal of non-welded and welded Ti-6Al-4V alloys with testing time in the non-stressed state and slow-strain-rate tensile test. The external

stress state has an obvious effect on the corrosion process of the sample. The slope of the PSD curve under the non-stressed state shows similar characteristics, and the slope is lower than -20 dB/dec. During the slow-strain-rate tensile test, the slope of the PSD curve is different from that under the non-stressed state, the slopes of the non-welded sample tested at 0~16 h and welded sample tested at 0~4 h is lower than -20 dB/dec, but they are higher than -20 dB/dec when the slow-strain-rate tensile test is performed for 20 h and 6 h.

Related studies have shown that the material is in a passivation state when the slope of the PSD curve is lower than -20 dB/dec, whereas values above -20 dB/dec indicate that a localized corrosion process has occurred in the material [38,64]. The slope of the non-stressed sample indicates that the surface state of the sample is relatively stable, and the surface is always in a stable passivation state during the immersion test, since the protective effect of the oxide film on the sample surface makes the corrosion medium have little effect on the sample, and the surface state of the sample remains basically unchanged [6-10]. For the samples with the slow-strain-rate tensile test, the slope shows that the surface states of the non-welded sample tested at 0~16 h and welded sample tested at 0~4 h are similar to that of the non-stressed sample, which indicates that no corrosion occurred on the sample surface [50]. As the slow-strain-rate tensile test proceeds, the surface stability of the non-welded sample tested at 20 h and welded sample tested at 6 h greatly decreases due to the continuous effect of the accumulated load and corrosion medium, which results in the corrosion process. Therefore, the slope indicates that localized corrosion occurred on the sample surface at this time [50,57,58].

4. CONCLUSIONS

In this study, electrochemical noise has been used to investigate the electrochemical behavior of Ti-6Al-4V alloy before and after the welding process under non-stressed state and slow-strain-rate tensile tests. For the non-welded and welded samples tested under the non-stressed state, the electrochemical noise resistance and absolute difference of the skewness coefficient and kurtosis coefficient of the current noise signal barely change during the immersion test, which indicates that the corrosion medium has little effect on the corrosion resistance of the sample. For the non-welded and welded samples in the slow-strain-rate tensile test, the electrochemical noise resistance gradually decreases, while the absolute difference of the skewness coefficient and kurtosis coefficient of the current noise signal gradually increases, which indicates that the corrosion resistance of the sample continuously deteriorates. For the non-welded and welded samples tested under the non-stressed state, the PSD curve slope of the current noise signal is below -20 dB/dec, which indicates that the sample surface is always in a stable passivation state. For the non-welded and welded samples tested in the slow-strain-rate tensile test, the PSD curve slope of the current noise signal of the non-welded sample tested at 0~16 h and welded sample tested at 0~4 h is lower than -20 dB/dec, which indicates the stable passivation state on the sample surface. When the slow-strain-rate tensile test is conducted for 20 h and 6 h, the PSD curve slope of the current noise signal of the non-welded sample and welded samples is higher than -20 dB/dec, which indicates that the localized corrosion process occurred on the sample surface. The welding process significantly reduces the corrosion resistance of the sample under the non-

stressed state and slow-strain-rate tensile test because of different properties of the oxide film on the sample surface before and after the welding process. The applied load enhances the electrochemical activity of the non-welded and welded samples, which leads to the high sensitivity of the sample in the corrosion medium.

References

1. M. Mihalikova, M. Hagarova, D. Jakubéczyová, J. Cervová and A. Lišková, *Int. J. Electrochem. Sci.*, 11 (2016) 4206.
2. R.M.A. Shahba, W.A. Ghannem, A.El-Sayed. El-Shenawy, A.S.I. Ahmed and S.M. Tantawy, *Int. J. Electrochem. Sci.*, 6 (2011) 5499.
3. J. Mendoza-Canales and J. Marín-Cruz, *Int. J. Electrochem. Sci.*, 3 (2008) 346.
4. F. El-Taib Heakal and Kh.A. Awad, *Int. J. Electrochem. Sci.*, 6 (2011) 6483.
5. C. Vasilescu, P. Drob, E. Vasilescu, P. Osiceanu, S.I. Drob and M.V. Popa, *Int. J. Electrochem. Sci.*, 8 (2013) 10733.
6. K.M. Ibrahim, M.M. Moustafa, M.W. Al-Grafi, N. El-Bagoury and M.A. Amin, *Int. J. Electrochem. Sci.*, 11 (2016) 3206.
7. S.X. Zhou, J. Wang and P. Cai, *Int. J. Electrochem. Sci.*, 12 (2017) 7174.
8. C.L. Huang, T.H. Chen, C.C. Chang and S.Y. Lin, *Int. J. Electrochem. Sci.*, 13 (2018) 2779.
9. H. Jiang, *Int. J. Electrochem. Sci.*, 13 (2018) 3888.
10. X.W. Chen, D.D. Liao, D.F. Zhang, X. Jiang, P.F. Zhao and R.S. Xu, *Int. J. Electrochem. Sci.*, 15 (2020) 710.
11. A.K. Roy, D.L. Fleming, D.C. Freeman and B.Y. Lum, *Micron*, 30 (1999) 649.
12. M.D. Pustode and S. Raja, *Metall. Mater. Trans. A.*, 46A (2015) 6081.
13. T.P. Chapman, V.A. Vonortsov, A. Sankaran, D. Rugg, T.C. Lindley and D. Dye, *Metall. Mater. Trans. A.*, 47A (2016) 282.
14. X.Z. Guo, K.W. Gao, W.Y. Chu and L.J. Qiao, *Mat. Sci. Eng. A-Struct.*, 346 (2003) 1.
15. Z. Qin, X.L. Pang, Y. Yan, L.J. Qiao, H.T. Tran and A.A. Volinsky, *Corros. Sci.*, 78 (2014) 287.
16. M. Enerenaz, P. Faure and J.A. Petit, *Corros. Sci.*, 40 (1998) 939.
17. S. Pao, D.A. Meyn, R.A. Bayles, C.R. Feng and G.R. Yoder, *Scripta Mater.*, 36 (1997) 1321.
18. D.J. Simbi and J.C. Scully, *Corros. Sci.*, 37 (1995) 1325.
19. M.H.O. Kiiniinen, E.T. Lavonius and J.K. Kivilahti, *Dent. Mater.*, 11 (1995) 269.
20. J. Liu, X.L. Gao, L.J. Zhang and J.X. Zhang, *Eng. Fract. Mech.*, 117 (2014) 84.
21. X.L. Gao, J. Liu, L.J. Zhang and J.X. Zhang, *Mater. Charact.*, 93 (2014) 136.
22. X. Cao and M. Jahazi, *Opt. Laser Eng.*, 47 (2009) 1231.
23. X.L. Gao, L.J. Zhang, J. Liu and J.X. Zhang, *Int. J. Adv. Manuf. Technol.*, 72 (2014) 895.
24. X.J. Cao, A.S.H. Kabir, P. Wanjara, J. Gholipour, A. Birur, J. Cuddy and M. Medraj, *Metall. Mater. Trans. A.*, 45A (2014) 1258.
25. M. Heidarbeigy, F. Karimzadeh and A. Saatchi, *Mater. Lett.*, 62 (2008) 1575.
26. Z. Han, H. Zhao, X.Y. Chen and H.C. Lin, *Mat. Sci. Eng. A-Struct.*, 277 (2000) 38.
27. F. Karimzadeh, M. Heidarbeigy and A. Saatchi, *J. Mater. Process. Tech.*, 206 (2008) 388.
28. M. Balasubramanian, V. Jayabalan and V. Balasubramanian, *Mater. Design*, 29 (2008) 1359.
29. S.P. Trasatti and E. Sivieri, *Mater. Chem. Phys.*, 83 (2004) 367.
30. H.V.S. Nayak, K.I. Vasu and Y.V.R.K. Prasad, *J. Mater. Sci.*, 15 (1980) 1265.
31. M.G. Pujar, T. Anita, H. Shaikh, R.K. Dayal and H.S. Khatak, *Int. J. Electrochem. Sci.*, 2 (2007) 301.
32. M.G. Pujar, K. Laha, R.K. Dayal and N. Shinya, *Int. J. Electrochem. Sci.*, 3 (2008) 891.
33. C.G. Nava-Dino, G. López-Ocaña, J.A. Cabral-Miramontes, M.A. Luna-Ramirez, H. Monreal-

- Romero, R. Bautista-Margulis, J.G. Chacon-Nava and A. Martinez-Villafane, *Int. J. Electrochem. Sci.*, 7 (2012) 11182.
34. X.H. Wang, J.H. Wang and X. Yue, *Int. J. Electrochem. Sci.*, 9 (2014) 6558.
35. M. Leban, V. Dolecek and A. Legat, *Corrosion*, 56 (2000) 921.
36. B. Malki, A. Legris, J.L. Pastol and D. Gorse, *J. Electrochem. Soc.*, 146 (1999) 3702.
37. Y. Watanabe and T. Kondo, *Corrosion*, 56 (2000) 1250.
38. G. Du, J. Li, W.K. Wang, C. Jiang and S.Z. Song, *Corros. Sci.*, 53 (2011) 2918.
39. C.S. Brossia, E. Gileadi and R.G. Kelly, *Corros. Sci.*, 37 (1995) 1455.
40. T. Kawai, H. Nishisara and K. Aramaki, *Corros. Sci.*, 37 (1995) 823.
41. T. Kawai, H. Nishisara and K. Aramaki, *Corros. Sci.*, 8 (1996) 225.
42. C.S. Brossia and R.G. Kelly, *Electrochim. Acta*, 41 (1996) 2579.
43. T. Kawai, H. Nishihara and K. Aramaki, *J. Electrochem. Soc.*, 143 (1996) 3866.
44. A. Torres-Islas and J.G. González-Rodríguez, *Int. J. Electrochem. Sci.*, 4 (2009) 640.
45. G. Yi and C.B. Zheng, *Int. J. Electrochem. Sci.*, 7 (2012) 10633.
46. Ihsan-ul-Haq. Toor, *Int. J. Electrochem. Sci.*, 9 (2014) 2737.
47. M.A. Espinosa-Medina, G. Carbajal-De la Torre, A. Sánchez-Castillo, C. Ángeles-Chávez, T. Zeferino-Rodríguez and J.G. González-Rodríguez, *Int. J. Electrochem. Sci.*, 12 (2017) 6952.
48. J.O. Yin, Y.S. Wu, J. Lu, B.F. Ding, L. Zhang and B. Cao, *Rare. Metal. Mat. Eng.*, 6 (2003) 436.
49. Y.S. Wu, Y.L. Jiang, H. Chu, Z.Y. Ding and B.F. Ding, *J. Univ. Sci. Technol. B.*, 1 (2003) 40.
50. Y. Liu, S.W. Tang, G.Y. Liu, Y. Sun and J. Hu, *Int. J. Electrochem. Sci.*, 11 (2016) 8530.
51. U. Bertocci, F. Huet, R.P. Nogueira and P. Rousseau, *Corrosion*, 58 (2002) 337.
52. A.M. Homborg, T. Tinga, X. Zhang, E.P.M. van Westing, P.J. Oonincx, J.H.W. de Wit and J.M.C. Mol, *Electrochim. Acta*, 70 (2012) 199.
53. B. Ramezanzadeh, S.Y. Arman, M. Mehdipour and B.P. Markhali, *Appl. Surf. Sci.*, 289 (2015) 129.
54. C. Gabrielli and M. Keddam, *J. Electroanal. Chem.*, 359 (1993) 1.
55. F. Mansfeld and H. Xiao, *Prog. Org. Coat.*, 30 (1997) 89.
56. C.C. Lee and F. Mansfeld, *Corros. Sci.*, 40 (1998) 959.
57. Y. Liu, S.W. Tang, G.Y. Liu, Y. Sun and J. Hu, *Int. J. Electrochem. Sci.*, 11 (2016) 10561.
58. Y. Liu, S.W. Tang, G.Y. Liu, Y. Sun and J. Hu, *Met. Mater. Int.*, 23 (2017) 488.
59. P.R. Roberge, *Corrosion*, 50 (1994) 506.
60. A.M. Naguib, *Chinese. J. Chem.*, 24 (2006) 247.
61. R.A. Cottis, A.M. Homborg and J.M.C. Mol, *Electrochim. Acta*, 202 (2016) 277.
62. U. Bertocci, F. Huet and B. Jaoul, *Corrosion*, 28 (1999) 2039.
63. Y.F. Cheng, M. Wilmott and J.L. Luo, *Corros. Sci.*, 41 (1999) 1245.
64. J.C. Uruchurtu and J.L. Dawson, *Corrosion*, 43 (1987) 19.